



TABLE I  
DETAILED DIMENSIONS (UNIT: mm)

$l_s$	$l_1$	$w_1$	$l_2$	$w_2$	$l_3$	$l_4$
75	16	16	10.1	0.2	12.6	8.3
$d$	$l_r$	$w_r$	$a_1$	$a_2$	$r_1$	$r_2$
34.5	3	1.3	3.3	1.8	3	1.2

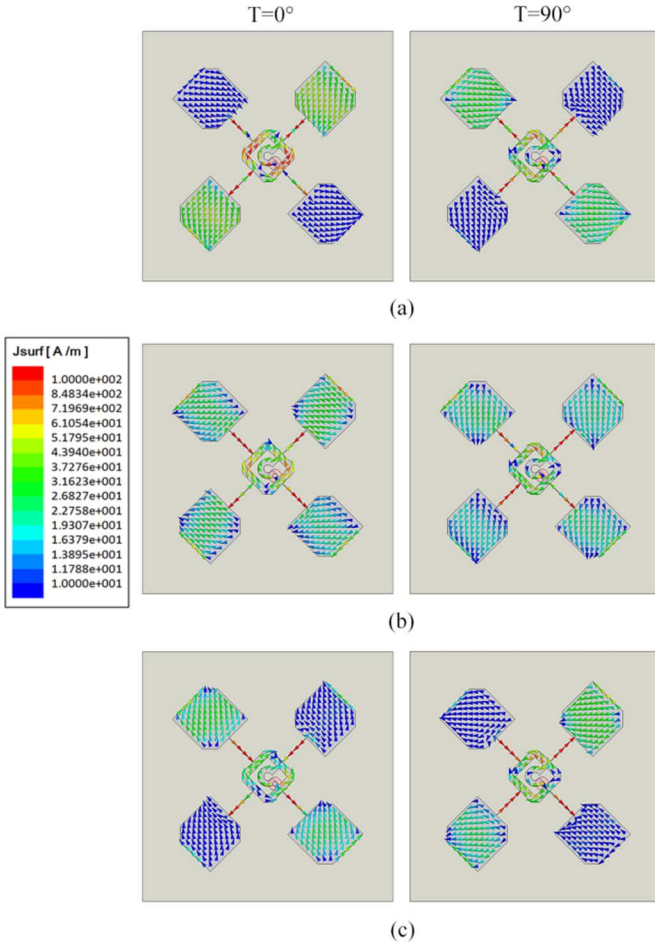


Fig. 2. Current distribution on the proposed array at different frequency: (a) 5.3 GHz, (b) 5.68 GHz, (c) 5.9 GHz.

wave simulator and the detailed values of each parameter are listed in Table I.

The center frequency of the proposed array is designed at 5.5 GHz and the effective wavelength is 41.2 mm, according to the equation  $\lambda_g = 2\lambda_0/(1 + \epsilon_r)$ . The sector of  $270^\circ$  has a mean arc length of about  $\lambda_g/4$ , which not only serves as an impedance transformer but also provides a phase difference of  $90^\circ$ . By connecting the sector and the loop via two strips, the loop's one-wavelength mode is excited and sequential phases of  $0^\circ$ ,  $90^\circ$ ,  $180^\circ$ , and  $270^\circ$  appear at the loop's four arms. The loop is extended by four  $\lambda_g/4$  strips, which are used to provide stable input impedance for the four arms of the loop. Taking the center frequency for example, the edge impedance of the patch elements is about  $120 + j30 \Omega$ , the characteristic impedance of the transformers is about  $180 \Omega$ . Thus, the input impedance via the  $\lambda_g/4$  transformer is about  $250 - j60 \Omega$ . Then, the four input impedances via the loop are transformed into about  $40 - j2 \Omega$ , which is well matched to  $50 \Omega$ .

In this communication, two LP modes and one CP mode of the patch elements are excited at different frequencies by truncating large cor-

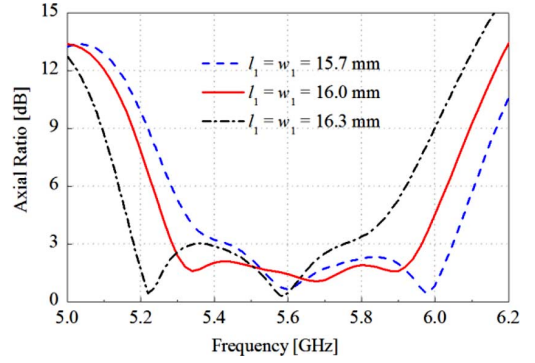


Fig. 3. Simulated AR of the proposed array with different element size.

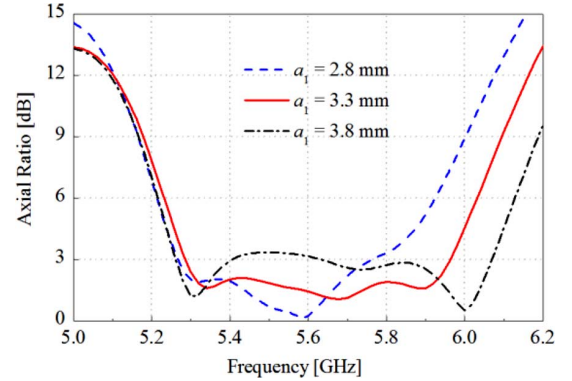


Fig. 4. Simulated AR of the proposed array with different  $a_1$ .

ners. Fig. 2 shows the current distribution on the array at different frequencies with different phases. In the low frequency, the resonance is mainly determined by the longer diagonal of the patch elements. In Fig. 2(a), it can be observed that a pair of elements on the diagonal of the array is excited at  $T = 0^\circ$ , and the other pair of elements is excited at  $T = 90^\circ$ . Moreover, the current directions in  $T = 0^\circ$  and  $90^\circ$  are orthogonal. Thus, the array is CP even though the elements are LP. A similar phenomenon is found in Fig. 2(c), where the resonance in the high frequency is determined by the shorter diagonal of the patch elements. In Fig. 2(b), it is shown that all the four elements are excited at the same time with consistent current directions at  $T = 0^\circ$ , and the current directions rotate  $90^\circ$  at  $T = 90^\circ$ . Thus, both the array and the elements are CP in the middle frequency. By combining the three CP operating modes at different frequencies, right-hand circular polarization (RHCP) is achieved in a broad bandwidth.

A parameter study is carried out to further verify the operating principle mentioned above. Fig. 3 shows the effect of elements' size on the AR performance of the array, which affects both the longer and shorter diagonals of elements. It can be observed that the AR curve moves downward with the increase of elements' size. Fig. 4 shows the effect of  $a_1$  on AR, which only affects the shorter diagonal of elements. It is shown that as  $a_1$  increases, the resonance in the high frequency shifts upward, while the resonance in the low frequency changes slightly. These results verify that the resonances in the low and high frequencies are determined by the longer and shorter diagonals of elements, respectively.

### III. EXPERIMENTAL RESULTS

Fig. 5 shows the prototype of the proposed  $2 \times 2$  patch array. The measured reflection coefficient of the array is shown in Fig. 6, which agrees well with the simulated result. The measured  $-10$ -dB reflection coefficient bandwidth is from 5.2 GHz to 6.23 GHz, or about

TABLE II  
A COMPARISON TABLE BETWEEN THE PROPOSED  $2 \times 2$  ARRAY AND OTHER SINGLE-LAYER  $2 \times 2$  ARRAYS

$2 \times 2$ arrays	[13]	[14]	[15]	[20]	Proposed
10-dB impedance bandwidth (%)	7.3	15.45	8	6	>19
3-dB AR bandwidth (%)	4.4	5.4	4.8	6.8	12.7
Total size ( $\lambda_g$ )	Not Given	$1.96 \times 1.96 \times 0.031$	$1.92 \times 1.92 \times 0.021$	$2.17 \times 2.17 \times 0.076$	$1.82 \times 1.82 \times 0.036$

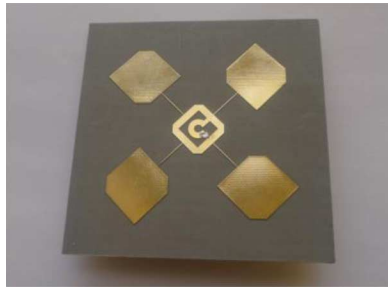


Fig. 5. Photograph of the fabricated  $2 \times 2$  patch array.

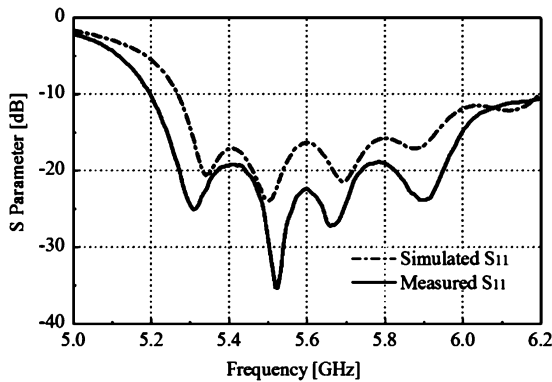


Fig. 6. Simulated and measured reflection coefficient of the  $2 \times 2$  array.

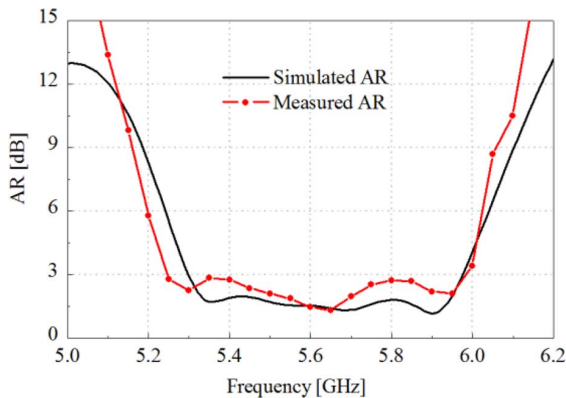


Fig. 7. Simulated and measured axial ratio of the  $2 \times 2$  array.

18.7% corresponding to the center frequency of 5.5 GHz. The fact that the measured results have smaller values than the simulated results is mainly attributed to dielectric loss and fabrication error. Fig. 7 shows the simulated and measured AR results. The measured 3-dB AR bandwidth of the array is from 5.25 GHz to 5.95 GHz, or about 12.7%, which is within the  $-10$ -dB reflection coefficient bandwidth. It can also be observed that the measured ARs below 3 dB vary a little larger than the simulated ones, and a wider AR bandwidth is achieved. This difference between simulation and measurement is caused by fabrication error and measurement error, also with uncertain permittivity of substrate.

Fig. 8 shows the simulated and measured gains. It is shown that the measured gain of the array is about 11.5-dBic in most of the 3-dB AR

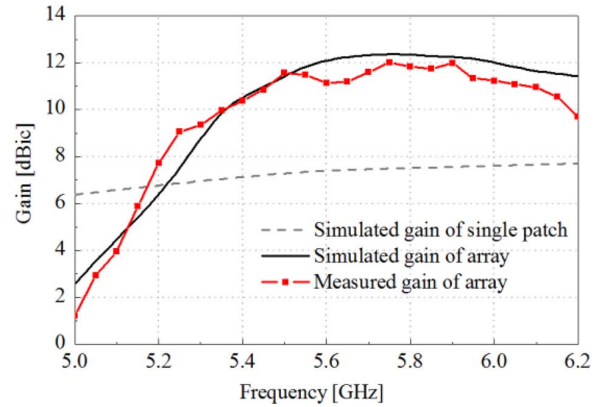


Fig. 8. Simulated and measured gains.

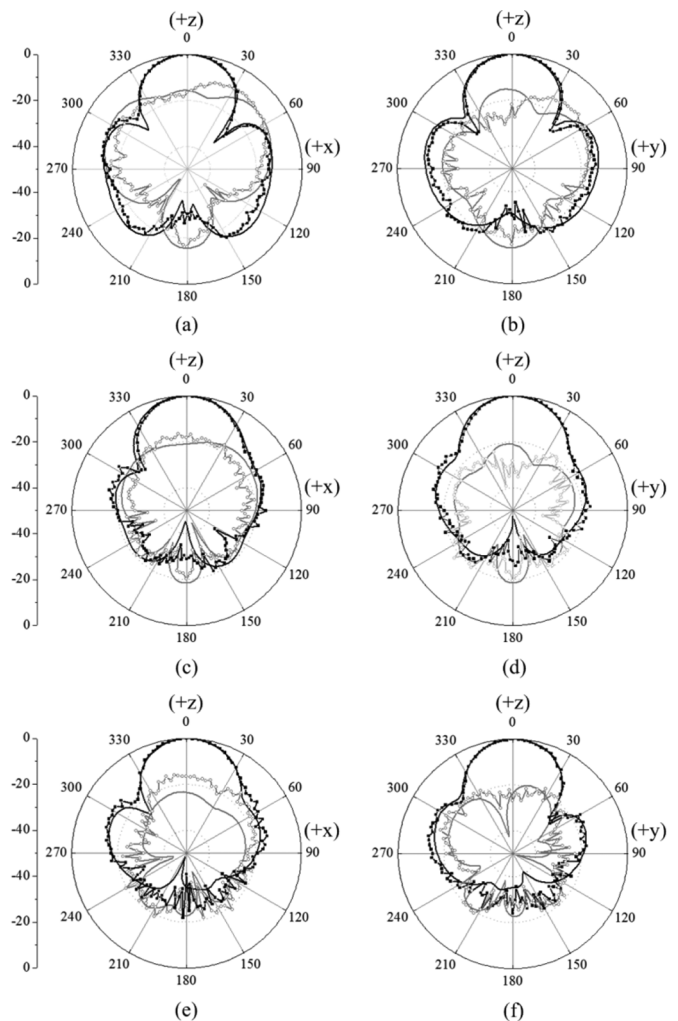


Fig. 9. Simulated and measured normalized radiation patterns of the  $2 \times 2$  array. (a),(b) 5.3 GHz; (c),(d) 5.6 GHz; (e),(f) 5.9 GHz.

bandwidth, which is about 4.5-dB higher than that of a single element. It is also observed that the gain in the low frequency drops fast with the

decrease of frequency. This is mainly caused by the limited bandwidth of the feeding network. The measured gain variation is less than 3 dB in the concerned 3 AR bandwidth and the measured peak gain is about 12 dBic at 5.75 GHz.

The simulated and measured normalized radiation patterns in the  $xz$ - and  $yz$ -planes at different frequencies are shown in Fig. 9. It is shown that the measured results agree well with the simulated results. The measured front-to-back ratio is better than 16 dB at 5.3 GHz, better than 20 dB at 5.6 GHz and 5.9 GHz. Also, the co-polarization (RHCP) gain at broadside is 17 dB higher than the cross-polarization (left-hand circular polarization, LHCP) gain at all the frequencies in both planes.

The comparison of the proposed patch array with other referenced single-layer  $2 \times 2$  arrays is listed in Table II. It is shown that the comprehensive bandwidth of the proposed array with  $S_{11} < -10$  dB,  $AR < 3$  dB, is double enhanced, when compared with other referenced single-layer  $2 \times 2$  patch arrays. Besides, the planar size of the proposed array is smallest among all the designs.

#### IV. CONCLUSION

A compact single-layer wideband CP  $2 \times 2$  patch array is proposed in this communication. Three operating modes of patch elements at different frequencies are analyzed and excited by using a sequential-phase feeding network. Both impedance and AR bandwidths are greatly enhanced by combining these three modes together, which can be tuned and matched by optimizing the truncated corners of elements and the sequential-phase feeding network. The measured bandwidth with  $S_{11} < -10$  dB,  $AR < 3$  dB is 700 MHz, or 12.7% corresponding to the center frequency, which is double wider than the previous published single-layer  $2 \times 2$  patch arrays. The measured peak gain is 12 dBic. In the band of 5.45–5.9 GHz, the gain is about 11.5 dBic, and the gain variation is less than 3 dB within the 3-dB AR bandwidth. The proposed  $2 \times 2$  patch array, with the advantages of single-layer structure, and wide AR bandwidth, is a promising candidate for CP array design.

#### REFERENCES

- [1] P. S. Hall, J. S. Dahele, and J. R. James, "Design principles of sequentially fed wide bandwidth circularly polarized microstrip antennas," in *Proc. Inst. Elect. Eng.*, Oct. 1989, vol. 136, pp. 381–389.
- [2] A. A. Kishk, "Performance of planar four elements array of single-fed circularly polarized dielectric resonator antenna," *Microw. Opt. Technol. Lett.*, vol. 38, no. 5, pp. 381–384, 2003.
- [3] R. Ramirez, F. Flaviis, and N. G. Alexopoulos, "Single-feed circularly polarized microstrip ring antenna and arrays," *IEEE Trans. Antennas Propag.*, vol. 48, no. 7, pp. 1040–1047, 2000.
- [4] H. Iwasaki, "A circularly polarized rectangular microstrip antenna using single-fed proximity-coupled method," *IEEE Trans. Antennas Propag.*, vol. 43, no. 8, pp. 895–897, Aug. 1995.
- [5] W. K. Lo, C. H. Chan, and K. M. Luk, "Circularly polarized microstrip antenna array using proximity coupled feed," *Electron. Lett.*, vol. 34, no. 23, pp. 2190–2191, Nov. 1998.
- [6] W. K. Lo, C. H. Chan, and K. M. Luk, "Circularly polarised patch antenna array using proximity-coupled L-strip line feed," *Electron. Lett.*, vol. 36, no. 14, pp. 1174–1175, July 2000.
- [7] J. W. Wu and J. H. Lu, " $2 \times 2$  circularly polarized patch antenna arrays with broadband operation," *Microw. Opt. Technol. Lett.*, vol. 39, no. 5, pp. 360–363, 2003.
- [8] L. Bian and X. Q. Shi, "Wideband circularly-polarized serial rotated  $2 \times 2$  circular patch antenna array," *Microw. Opt. Technol. Lett.*, vol. 49, no. 12, pp. 3122–3124, 2007.
- [9] Y. Lu, D. G. Fang, and H. Wang, "A wideband circularly polarized  $2 \times 2$  sequentially rotated patch antenna array," *Microw. Opt. Technol. Lett.*, vol. 49, no. 6, pp. 1405–1407, 2007.
- [10] K. H. Lu and T.-N. Chang, "Circularly polarized array antenna with corporate-feed network and series-feed elements," *IEEE Trans. Antennas Propag.*, vol. 53, no. 10, pp. 3288–3292, 2005.
- [11] J. Janapsatya, Nasimuddin, and K. P. Esselle, "Jawidening the bandwidth of single-fed circularly polarized microstrip patch antenna using sequential array," in *Proc. Antennas Propag. Soc. (AP-S) Int. Symp.*, Jul. 2008, pp. 1–4.
- [12] E. T. Rahardjo, S. Kitao, and M. Haneishi, "Circularly polarized planar antenna excited by cross-slot coupled coplanar waveguide feedline," in *Proc. Antennas Propag. Soc. Int. Symp. Dig.*, 1994, vol. 3, pp. 2220–2223.
- [13] I. J. Chen, "CPW-fed circularly polarized  $2 \times 2$  sequentially rotated patch antenna array," in *Microw. Conf. Proc. (APMC)*, 2005, vol. 4.
- [14] A. Chen, Y. Zhang, Z. Chen, and S. Cao, "A Ka-band high-gain circularly polarized microstrip antenna array," *IEEE Antennas Wireless Propag. Lett.*, vol. 9, pp. 1115–1118, 2010.
- [15] S. Lin and Y. Lin, "A compact sequential-phase feed using uniform transmission lines for circularly polarized sequential-rotation arrays," *IEEE Trans. Antennas Propag.*, vol. 59, no. 7, pp. 2721–2724, 2011.
- [16] K. K. Pang, H. Y. Lo, K. W. Leung, K. M. Luk, and E. K. N. Yung, "Circularly polarized dielectric resonator antenna subarrays," *Microw. Opt. Technol. Lett.*, vol. 27, no. 6, pp. 377–379, Dec. 2000.
- [17] S. L. S. Yang, R. Chair, A. A. Kishk, K. F. Lee, and K. M. Luk, "Study on sequential feeding networks for sub-arrays of circularly polarized elliptical dielectric resonator antenna," *IEEE Trans. Antennas Propag.*, vol. 55, no. 2, pp. 321–333, Feb. 2007.
- [18] S. Yang, R. Chair, A. A. Kishk, K. F. Lee, and K. M. Luk, "Circular polarized elliptical dielectric resonator antenna sub array fed by hybridizing feeding network," in *Proc. IEEE Int. Symp. Antennas Propag.*, Jul. 2006, pp. 2221–2224.
- [19] J. Huang, "A technique for an array to generate circular polarization using linearly polarized elements," *IEEE Trans. Antennas Propag.*, vol. 34, no. 9, pp. 1113–1124, Sep. 1986.
- [20] Y. Li, Z. Zhang, and Z. Feng, "A sequential-phase feed using a circularly polarized shorted loop structure," *IEEE Trans. Antennas Propag.*, vol. 61, no. 3, pp. 1443–1447, 2013.